R.E.M. (Rekayasa Energi Manufaktur) Jurnal | Vol.10 No.2/2025
ISSN online (2528-3723)
http://doi.org/10.21070/rem.v10i2.1792

Observe the Response a Finite Element Linear Static Analysis Simulation Was Conducted on the Fire Extinguisher Refill Frame

Rizki Aulia Nanda[1*], Karyadi[1], Dodi Mulyadi[1], Ade Suhara[2]
*Email corresponding author: rizki.aulianda@ubpkarawang.ac.id

[1]Mechanical Engineering, Universitas Buana Perjuangan Karawang, Karawang, Jawa Barat, Indomesia
[2]Industrial Engineering, Universitas Buana Perjuangan Karawang, Karawang, Jawa Barat, Indomesia

Article history: Received: 2 November 2025 | Revised: 27 November 2025 | Accepted: 4 Desember 2025

Abstract. *The apar refill machine consists of several components so that the frame of the apparatus requires a strength analysis of the frame. The problem that arises to make a portable apparatus is that there are 2 main components that depend and 1 component that does not depend, so the purpose of this study is with the process of finite element linear static analysis, the results of the frame design can show the reactions that arise due to the existing load, whether the frame is safe to use or not. This research method begins with design, material input, mesh input, boundary condition input and force input. The results show that the reactions that occur are the highest stress of 18,882 N, disspacement 2,450E + 00 mm, strain of 8,182E-05 and safety factor 11,931. From these results, according to the mechanical properties reference static linear threshold, the value is still safe at the maximum force threshold.*

Keywords - *Finite Element; Static Liniear; Chasis; Safety Factor*

INTRODUCTION

A fire extinguisher (APAR) functions as a rapid-response tool for extinguishing fires. However, once used, the extinguisher becomes depleted and must be refilled. This study designs a frame capable of supporting several components required for the refilling process. Since the refilling operation must be portable—allowing movement from one point to another—an efficient and flexible design is essential. Designing a flexible refilling station, however, presents challenges, as certain components must be suspended. For example, the funnel section must hang to ensure proper alignment between the funnel nozzle and the extinguisher nozzle. Similarly, the vacuum blower is positioned at the back and suspended, which creates additional load on the frame. Therefore, the research problem focuses on determining how the refilling frame structure can withstand these loads and evaluating the material's safety level to prevent potential failure during real operation. To determine the safety factor of the design, a linear static simulation is required to obtain the structural response under loading. This study also refers to previous research that conducted static analysis using simulation software to obtain the resulting reaction values[1]. The purpose of the static analysis simulation is to observe the structural reactions that occur when a load mass is applied to the frame supporting all the components. The frame responds automatically based on mathematical calculations without the need for manual computation. To conduct the finite element simulation test, a 3D model design is required using CAD software. Designing the 3D model with CAD provides a precise representation along the X, Y, and Z axes. From these axes, it becomes possible to calculate the structural reactions that occur when the components are subjected to loading[2]. These reactions must be accompanied by the provision of materials, loads, supports and mesh[3][4][5]. The force exerted is the influence of mass due to gravity which can be seen in equation 1[6].

$$F = W \times g \quad (1)$$

From equation 1 it can be explained that F is force (N), W is mass (kg) and g is gravity (m/s^2)[7]. The force equation is applied as the load condition in the static analysis simulation. The next step is to determine the material to be used in the simulation process. Material selection is a crucial step because it serves as a reference for observing structural reactions different materials will produce different responses under the same loading conditions[8][9][10]. After determining the material, it is also necessary to determine the support or Boundary Condition which aims to see the support points of the frame[11]. And the last input is to set the mesh size to be small parts to calculate the reactions that appear[12]. So the reactions that appear are stress, strain, displacement and safety factor[13][14][15].

The stress value that appears is a derivative of the basic stress equation which can be seen in Equation 2.

$$\sigma = \frac{F}{A} \tag{2}$$

The resulting stress is σ which is the symbol for stress (MPa), F is the force (N) and A is the cross-sectional area. (m^2)[16]. Next is the displacement equation which can be seen in equation 3.

$$u = \frac{F \cdot L}{A \cdot E} \tag{3}$$

Displacement is a change in a material structure due to the load that occurs, therefore U is the displacement (mm), F is the axial force (N), L is the element length, A is the cross-sectional area, and E is the modulus of elasticity. This equation is often used to verify truss rod/element models in FEA[17][18]. As a result of changes in the shape of the structure, strain also occurs using equation 4..

$$\varepsilon\% = \frac{L - L0}{Lo} \tag{4}$$

Strain is a measure of the local deformation of a material — it indicates how much the distance between two material particles changes relative to its initial condition. The variable *L* represents the change in length (mm), while L_o denotes the original length (mm), and $\varepsilon\%$ expresses the percentage of strain that occurs. The final equation presented is used to calculate the safety factor value, as shown in Equation (5)[2][19].

$$N = \frac{R}{s} \tag{5}$$

To calculate the safety factor, you can see that N is the safety factor value, R is the maximum strength of the material (yield or ultimate) and S is the maximum stress, force, moment or load that has been calculated[20]. The literature review of previous studies discusses that, during static analysis calculations using finite element simulation, Equations (1) to (5) serve as the fundamental basis for obtaining the resulting reaction values. Accordingly, this study shares similarities with prior research; however, it introduces a research gap identified from the reviewed references. The first gap lies in the design phase—previous studies have focused solely on frames for fire extinguisher recharging systems, and no other articles have specifically analyzed the frame structure of fire extinguisher recharging units. The second gap involves the use of one variable input variable and two constant input variables, which is the novelty of this study. Based on the problems and background described previously, the purpose of this study is to utilize finite element simulations to determine the reaction values caused by the applied loads and identify the locations of these reactions, thereby assessing whether the fire extinguisher recharging frame is structurally sound for use. The novelty of this study lies in the design concept, which shows several supports used to support the fire extinguisher recharging hopper and a hanging support on the vacuum machine section to observe the reactions that occur.

METHOD

This research method discusses the stages undertaken to obtain the ideal strength value for the frame used in the fire extinguisher refilling process. The ideal result is represented by the material's safety factor value. Refer to Figure 1 to observe the research flow.

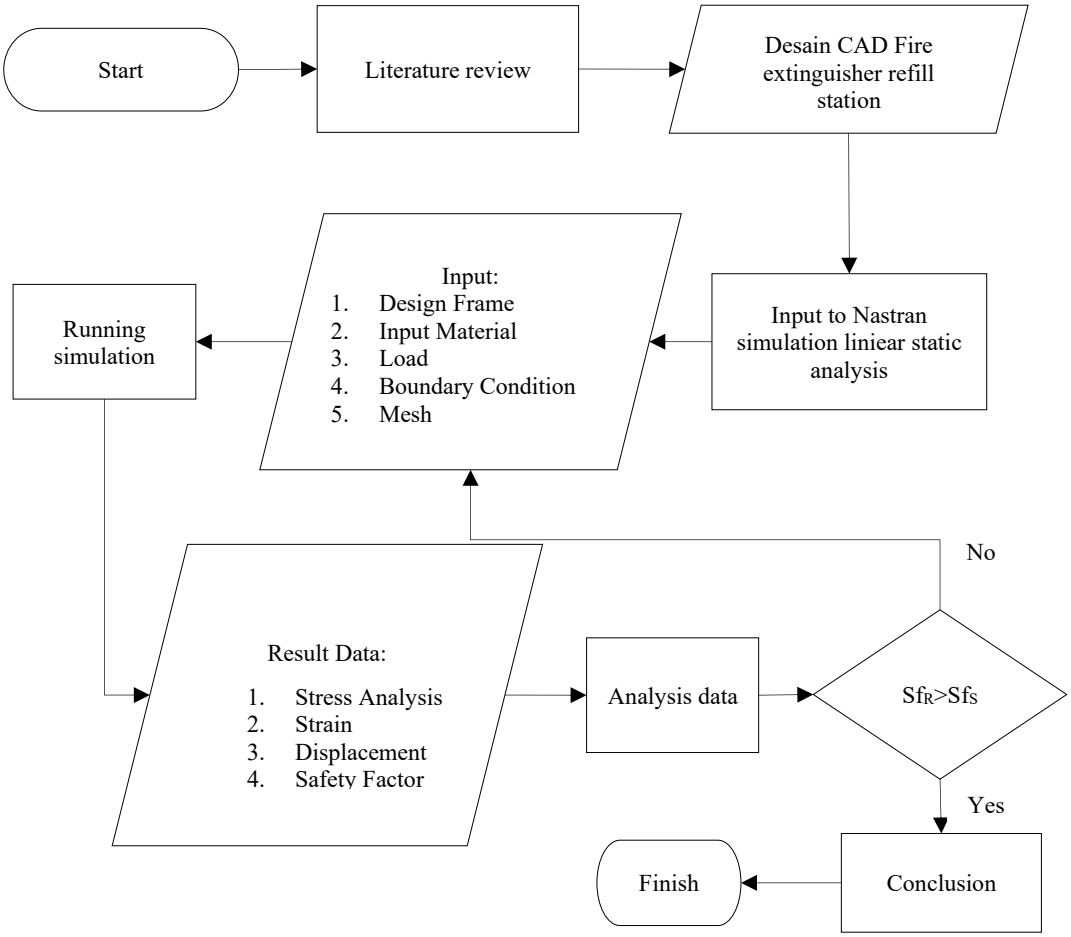

Figure 1. Research Flow

The research stages described in Figure 1 require a CAD drawing of the entire fire extinguisher refill product. The device consists of six main components, as shown in Figure 2.

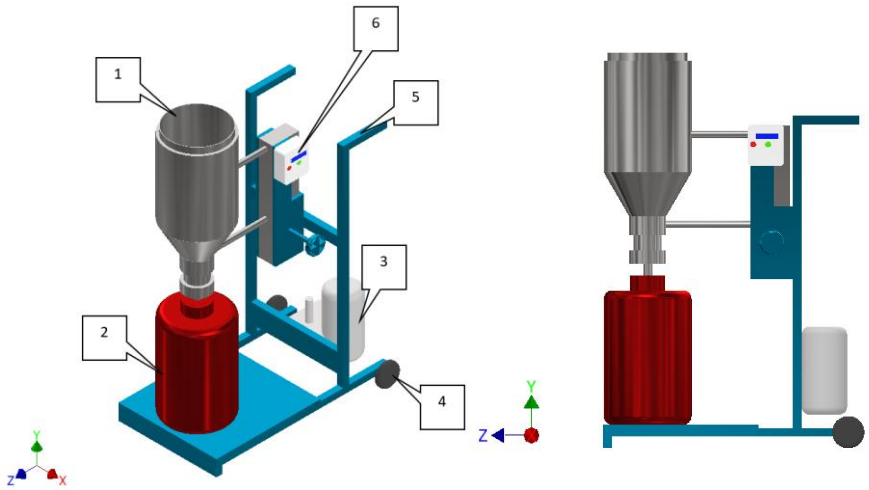

Figure 2. Design of the fire extinguisher refilling machine

Each component in Figure 2 can be seen using numbering symbols. Each component has its own function and has a different mass. Therefore, the components and their functions can be seen in Table 1.

Table 1. List of components

No	Component Name	Function
1	Refill funnel	functions as a container for the contents of the fire extinguisher which can be refilled via the nozzle (the contents of the fire extinguisher are CO_2 fire extinguishers)
2	Fire Extinguisher Tube	Functions as a container for fire extinguishers that will be refilled
3	Vacum Blower	The function of the vacuum is to hold pressure so that the CO_2 that is being filled does not overflow.
4	Wheel	As a mover when moved
5	Chassis	The frame is the support for all components, and this part will be analyzed to see the reactions that occur.
6	Control Panel	The control panel has the function of controlling on, off and emergency for the fire extinguisher refill tool.

From Table 1, which describes the components and their functions, the critical parts to be analyzed are the frame section of the fire extinguisher cylinder, the vacuum blower support, and the funnel refilling holder. An illustration of these components can be seen in Figure 3.

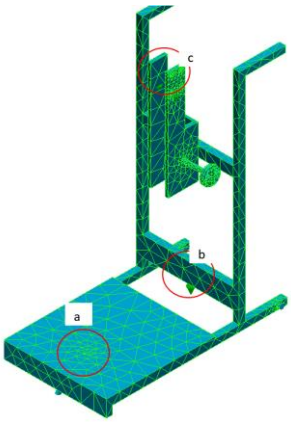

Figure 3. Determination of critical point (Load)

Each position identified as a critical point receives the corresponding force as illustrated in Figure 3. Point *a* represents the force exerted by the fire extinguisher, point *b* represents the force from the vacuum blower, and point *c* represents the force acting on the refilling funnel holder. The varying force is applied at point *a*, while constant forces are applied at points *b* and *c*. The detailed values of each applied force are presented in Table 2.

Table 2. Force Input

Position	Input Force (N)
a	49
	58,8
	88,2
b	246
c	456

The position shown in Figure 3 and the force shown in Table 2 obtained at position a are 3 variations of force originating from the mass of the apparatus multiplied by gravity consisting of an apparatus with a mass of 5 kg, an apparatus with a mass of 6 kg and a force of 9 kg. In Figure 3, a mesh input with a size of 63.8545 mm has also been carried out. The material used is Galvanized Steel with material specifications can be seen in Table 3.

Table 3. Galvanized Steel material specifications [21]

Mechanical Properties	Unit	Value
Yield strength	MPa	235 MPa
Tensile strength	MPa	510 MPa
Elongation (A, % pada patah)	%	26%
Young's modulus (E)	GPa	210 GPa

After inputting the design, load, material, and mesh, the final stage is to determine the supports used by the frame. The supports serve as the main foundation for maintaining the material's position and stability. The placement of the supports, or boundary conditions, can be seen in Figure 4.

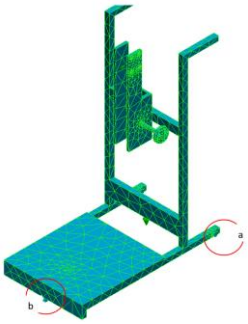

Figure 4. Boundary Condition

Two types of supports are used according to their respective functions: point *a* represents a roller support, while point *b* represents a frictional support that resists sliding motion. After all the input parameters are defined, the next stage is to run the simulation using the Autodesk Inventor Nastran application (Student Version).

RESULTS AND DISCUSSION

Based on the methodology described in the previous subsection, the results of this study present the outcomes of a finite element simulation. The main analysis results include Stress Analysis, Strain, Displacement, and Safety Factor. The first test was conducted with an applied load of 49 N, and the results are shown in Figure 5.

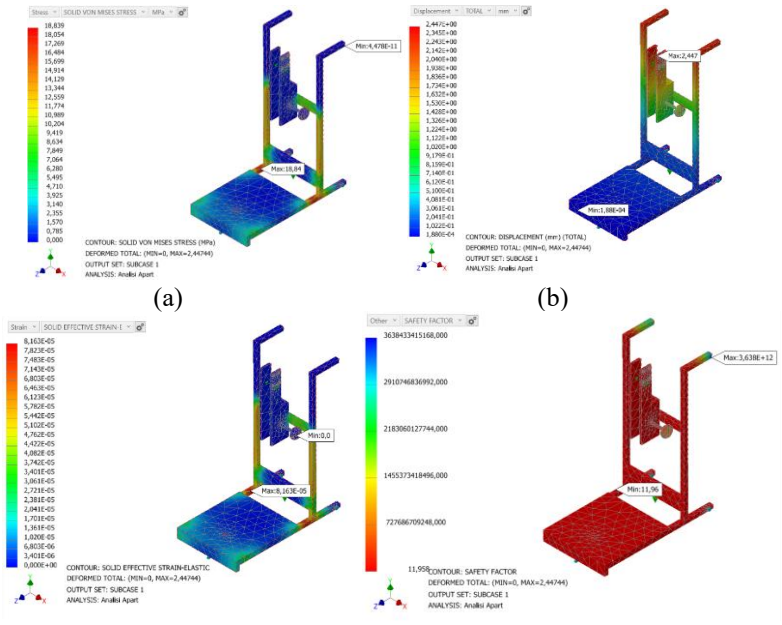

Figure 5. Simulation results at a force of 49 N

The results of the static analysis simulation can be explained as follows. Figure 5(a) shows the maximum stress value of 18.839 MPa, located at the area marked “Max: 18.84.” The red color indicates the region experiencing the highest stress concentration. Next, Figure 5(b) illustrates the displacement results, where the maximum displacement occurs at the top section of the funnel holder, marked as “Max: 2.447.” The largest displacement value is 2.447E+00 mm, indicating that the deformation is relatively insignificant. Figure 5(c) presents the strain distribution, with a maximum strain value of 8.163E-05 located at the region marked “Max: 8.63E-05.” The strain position corresponds closely to the stress concentration area shown in Figure 5(a). Finally, Figure 5(d) shows the safety factor results. The simulation indicates a maximum safety factor value of 11,958 located at the handle section of the frame, and a minimum safety factor value of 11.958. After determining the stress, displacement, strain, and safety factor values, the next simulation was performed with a load of 58.8 N, as shown in Figure 6.

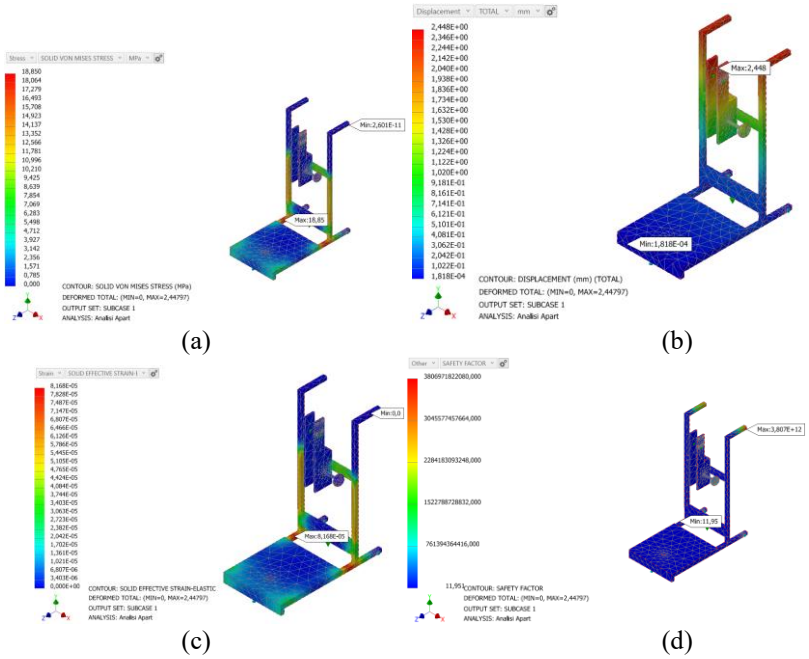

Figure 6. Simulation results at a force of 58.8 N

The simulation results for the applied load of 58.8 N are shown in Figure 6. Figure 6(a) illustrates an increase in stress, reaching a maximum value of 18.850 MPa, located at the same position as in the previous test. The red region again indicates the area of highest stress concentration. Figure 6(b) shows the displacement distribution, with the same reaction location but a slightly higher maximum displacement value of 2.448E+00 mm. Figure 6(c) presents the strain results, showing the same location of maximum strain with a value of 8.168E-05. Finally, Figure 6(d) shows the safety factor results, where the highest value occurs at the handle section with a magnitude of 11,951. The next simulation was performed with the highest applied load of 88.2 N, as shown in Figure 7.

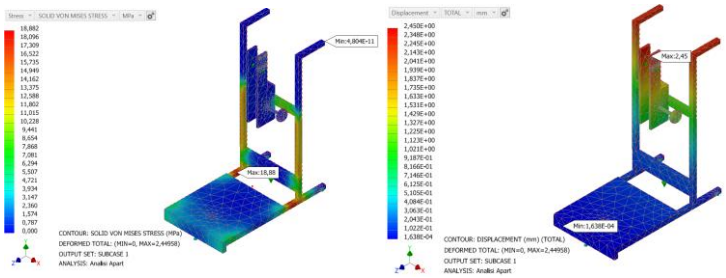

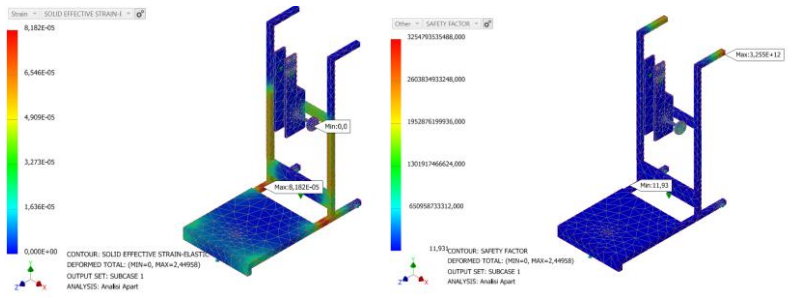

(c) (d)

Figure 7. Simulation results at a force of 88.2 N

The final simulation was conducted with an applied load of 88.2 N, as shown in Figure 7. Figure 7(a) illustrates the maximum stress value of 18.882 MPa, occurring at the same reaction location as in the previous simulations. Figure 7(b) shows the displacement results, with a maximum displacement value of 2.450E+00 mm at the same position. The maximum strain value, shown in Figure 7(c), is 8.182E-05, also located at the same reaction area. Lastly, Figure 7(d) presents the safety factor distribution, with the safety factor value of 11,931. Therefore, Figures 5, 6, and 7 collectively illustrate the critical reaction points that must be considered in the analysis. However, the structural feasibility of the frame must still be evaluated. Table 4 provides a summary of all the simulation results.

Table 4. Summary of Simulation Results

Indikator	49 N	58,8 N	88,2 N
Stress (MPa)	18,839	18,850	18,882
Displacement (mm)	2,447E+00	2,448E+00	2,450E+00
Strain	8,163E-05	8,168E-05	8,182E-05
Safety Factor	11,958 (MIN)	11,951 (MIN)	11,931(MIN)

The summary of the simulation results for the applied loads of 49 N, 58.8 N, and 88.2 N corresponds to the mass of fire extinguishers commonly available on the market, namely 5 kg, 6 kg, and 9 kg, respectively. The stress values increase proportionally with the applied load—the greater the load, the higher the stress produced. The maximum stress obtained is 18.882 MPa, with an average stress value of 18.893 MPa. The displacement values also increase with the applied load, where the maximum displacement recorded is 2.450E+00 mm, and the average displacement is 2.448E+00 mm. Similarly, the strain values show an increasing trend with higher applied loads, with a maximum strain of 8.182E-05 and an average strain of 8.171E-05.Finally, the safety factor behaves inversely, decreasing as the applied load increases. The lowest safety factor obtained is 11,931. However, these safety factor values must be compared with the standard mechanical properties established by ISO standards, which state that the safety factor for light static loads ranges between 1.5 and 2[22]. When compared with the standard range, the obtained safety factor value of 11,931 is still within a safe range and well above the minimum threshold. This study shows similarities with the research conducted by Agus Widyianto *et al.*, which analyzed the eSAF frame simulation using the finite element method to observe the resulting structural reactions. The results of this study indicate that as the applied load increases, the safety factor of the frame material decreases. However, the reduction in the safety factor does not affect the structural integrity as long as the obtained values remain significantly higher than the threshold specified in the mechanical property standards [9].

CONCLUSION

The conclusions drawn from this study are consistent with the research objectives. The applied loads were determined based on the typical capacities of fire extinguishers commonly used in the market, namely 5 kg, 6 kg, and 9 kg, corresponding to loads of 49 N, 58.8 N, and 88.2 N, respectively. In addition, other loads were applied, including 246 N on the funnel and 456 N on the vacuum blower. The load locations for the three variations were positioned at the center of the fire extinguisher placement area, on the vertical slider section for the funnel filling mechanism, and on the chassis for the vacuum blower. Two types of supports were used—two roller supports and one frictional support at the front section. The simulation results indicate that the stress and strain reactions are concentrated in the red-highlighted regions located on both sides of the fire extinguisher frame connectors. The displacement occurs primarily at the upper handle section and the funnel slider holder. The highest safety factor is observed in the storage section, while the lowest occurs at the handle area. The maximum stress value was obtained

under the 88.2 N load condition, with a displacement of 2.450E+00 mm and a strain of 8.182E-05. Conversely, the maximum safety factor value reached 3.638E+12. According to the standard safety factor criteria, these results indicate that the frame remains within the safe operating limit, as the values are still far above the minimum threshold, with the maximum reaction located at the handle section.

ACKNOWLEDGEMENT

This research was funded by the publication section and LPPM UBP Karawang, therefore we as authors express our gratitude for the financial assistance that has been provided.

REFERENCES

[1] T. T. T. Van, N. D. Tung, and N. Trung Kien, "Finite element analysis of plane frame systems with different models of semi-rigid connections," *IOP Conf. Ser. Mater. Sci. Eng.*, vol. 962, no. 2, 2020, doi: 10.1088/1757-899X/962/2/022060.

[2] M. L. Shreeshail, B. Santosh, R. C. Gireesha, G. U. Raju, G. K. Krishnaraja, and B. B. Kottursheṭtar, "Finite Element Analysis of Light Motor Vehicle Subframe for Mass Optimization," *AIP Conf. Proc.*, vol. 2446, no. May 2023, 2022, doi: 10.1063/5.0108555.

[3] D. Alvarado, E. Flores, and E. Paipa, "Design and validation by the finite element method of the structural arrangement of a riverine low draft combat boat," *Cienc. y Tecnol. buques*, vol. 15, no. 29, pp. 21–35, 2021, doi: 10.25043/19098642.218.

[4] J. Töpler, L. Buchholz, J. Lukas, and U. Kuhlmann, "Guidelines for a Finite Element Based Design of Timber Structures and Their Exemplary Application on Modelling of Beech LVL," *Buildings*, vol. 13, no. 2, 2023, doi: 10.3390/buildings13020393.

[5] M. Sakakibara, M. Ouchi, and H. Shirahata, "Analysis of bridges by finite element method and application of digital twin," *Life-Cycle Perform. Struct. Infrastruct. Syst. Divers. Environ.*, pp. 417–424, 2025, doi: 10.1201/9781003595120-50.

[6] D. Satrijo, O. Kurdi, and S. Wijaya, "Static Linear Stress Analysis of Road Bike Frame Design Using Finite Element Method," *Proc. Conf. Broad Expo. to Sci. Technol. 2021 (BEST 2021)*, vol. 210, no. Best 2021, pp. 430–433, 2022, doi: 10.2991/aer.k.220131.065.

[7] K. Zhu *et al.*, *Finite Element Software Analysis of Engineering Structure Test and Teaching Reform of Integration of Production and Teaching*. Atlantis Press International BV, 2023. doi: 10.2991/978-94-6463-172-2_180.

[8] L. Antonio, F. De Souza, and L. L. Verdade, "NUMERICAL-COMPUTATIONAL MODEL FOR DYNAMIC NONLINEAR ANALYSIS OF FRAMES WITH SEMI-RIGID CONNECTION CONSIDERING THE DAMPING EFFECT 1 INTRODUCTION Due to recent advances in computational resources , new possibilities are opened for the dynamic analysis of so," *RGSA – Rev. Gestão Soc. e Ambient. ISSN*, vol. 18, no. 1, pp. 1–19, 2024.

[9] A. Widyianto, Y. Budiman, R. Agistya, and N. Naila, "Results in Engineering Optimizing enhanced smart architecture frame (eSAF) topology : A computational approach to weight and strength trade-offs," *Results Eng.*, vol. 28, no. October, p. 107614, 2025, doi: 10.1016/j.rineng.2025.107614.

[10] Y. Li, Y. Deng, and A. Li, "A practical finite element simulation method for the Tuned Liquid Damper (TLD) in the entire structure," *J. Eng. Res.*, vol. 13, no. 3, pp. 2171–2178, 2025, doi: 10.1016/j.jer.2024.08.005.

[11] S. Mozaffari, M. Akbarzadeh, and T. Vogel, "Graphic statics in a continuum: Strut-and-tie models for reinforced concrete," *Comput. Struct.*, vol. 240, p. 106335, 2020, doi: 10.1016/j.compstruc.2020.106335.

[12] I. Bouckaert, M. Godio, and J. Pacheco de Almeida, "A Hybrid Discrete-Finite Element method for continuous and discontinuous beam-like members including nonlinear geometric and material effects," *Int. J. Solids Struct.*, vol. 294, no. April 2023, 2024, doi: 10.1016/j.ijsolstr.2024.112770.

[13] P. Azhir, J. Asgari Marnani, M. Panji, and M. S. Rohanimanesh, "A Coupled Finite-Boundary Element Method for Efficient Dynamic Structure-Soil-Structure Interaction Modeling," *Math. Comput. Appl.*, vol. 29, no. 2, 2024, doi: 10.3390/mca29020024.

[14] J. Szafran, K. Juszczyk-Andraszyk, and P. Kaszubska, "Effectiveness Analysis of the Non-Standard Reinforcement of Lattice Tower Legs Using the Component-Based Finite Element Method," *Materials (Basel).*, vol. 18, no. 6, 2025, doi: 10.3390/ma18061242.

[15] K. Khutal, G. Kathiresan, K. Ashok, B. Simhachalam, and D. Davidson Jebaseelan, "Design Validation Methodology for Bicycle Frames Using Finite Element Analysis," *Mater. Today Proc.*, vol. 22, pp. 1861–1869, 2019, doi: 10.1016/j.matpr.2020.03.085.

[16] S. Szirbik and Z. Virág, "Finite Element Analysis of a Steel Bridge Frame for Belt Conveyors," *Geosci. Eng.*, vol. 11, no. 1, pp. 110–116, 2023, doi: 10.33030/geosciences.2023.01.009.

[17] N. Qosim, Z. F. Emzain, A. M. Mufarrih, R. Monasari, F. Kusumattaqiin, and R. E. Santoso, "Finite Element Analysis of Ss316L-Based Five-Hole Plate Implant for Fibula Reconstruction," *J. Appl. Eng. Technol. Sci.*, vol. 4, no. 1, pp. 16–23, 2022, doi: 10.37385/jaets.v4i1.533.

[18] R. A. Nanda, A. Arhami, and R. Kurniawan, "Perancangan Dan Pengujian Model Mobil Robot Penanam Bibit Kangkung," *Rona Tek. Pertan.*, vol. 13, no. 2, pp. 14–28, 2020, doi: 10.17969/rtp.v13i2.16982.

[19] R. A. Nanda, T. Supriyono, R. A. R. Ma'arof, and F. M. Dewadi, "Analisis Chassis Mobil Robot Penanaman Bibit Kangkung Menggunakan Metode Elemen Hingga," *J. Tek. Mesin Mech. Xplore*, vol. 2, no. 2, pp. 1–8, 2022.

[20] U. Deep Kamal and R. Ranjan, "Finite Element Analysis of rigid plane frame and its application in Building Structures," no. April, pp. 0–5, 2023, [Online]. Available: https://www.researchgate.net/publication/370134493

[21] M. Šmak, J. Kubíček, J. Kala, K. Podaný, and J. Vaněrek, "The influence of hot-dip galvanizing on the mechanical properties of high-strength steels," *Materials (Basel).*, vol. 14, no. 18, pp. 1–19, 2021, doi: 10.3390/ma14185219.

[22] J. Tremblay *et al.*, *Shigley's Mechanical Engineering Design*, vol. 1, no. 1. 2016. [Online]. Available: http://www.biblioteca.pucminas.br/teses/Educacao_PereiraAS_1.pdf%0Ahttp://www.anpocs.org.br/portal/publicacoes/rbcs_00_11/rbcs11_01.htm%0Ahttp://repositorio.ipea.gov.br/bitstream/11058/7845/1/td_2306.pdf%0Ahttps://direitoufma2010.files.wordpress.com/2010/

This page is intentionally left blank